

Article

Optimization of Clove Oil Nanoemulsions: Evaluation of Antioxidant, Antimicrobial, and Anticancer Properties

José Nabor Haro-González ¹, Brenda Nathalie Schlienger de Alba ¹, Moisés Martínez-Velázquez ²,
Gustavo Adolfo Castillo-Herrera ¹ and Hugo Espinosa-Andrews ^{1,*}

¹ Unidad de Tecnología Alimentaria, Centro de Investigación y Asistencia en Tecnología y Diseño del Estado de Jalisco (CIATEJ), Camino Arenero # 1227, Col. El Bajío del Arenal, Zapopan 45019, Mexico; jose_nabor_94@hotmail.com (J.N.H.-G.); brdealba_al@ciatej.edu.mx (B.N.S.d.A.); gcastillo@ciatej.mx (G.A.C.-H.)

² Unidad de Biotecnología Médica y Farmacéutica, Centro de Investigación y Asistencia en Tecnología y Diseño del Estado de Jalisco (CIATEJ), Av. Normalistas 800, Col. Colinas de la Normal, Guadalajara 44270, Mexico; mmartinez@ciatej.mx

* Correspondence: hespinosa@ciatej.mx; Tel.: +52-3333455200 (ext. 1230)

Abstract: Clove essential oil is traditionally used as an anesthetic, analgesic, or insecticide, and recently, its applications as an antimicrobial, antioxidant, or anticancer agent have been explored. Nanoemulsions are thermodynamically unstable dispersions ($d < 100$ nm) produced by mixing two immiscible phases, which, in many cases, improve the stability and biological activities of functional ingredients for pharmaceutical, cosmetic, or food applications. This research optimized the formation of clove essential oil nanoemulsions by employing response surface methodology. The surfactant concentration was minimized by modifying the percentage of clove oil (0–100%), surfactant content (1–4%), and oil phase content (0–20%). In the optimum conditions, a nanoemulsion (93.19 ± 3.92 nm) was produced using 1.0% surfactant and 2.5% oil phase of which 50.7% was clove essential oil. The optimized nanoemulsion was stable in rapid stability tests (centrifugation, freezing–thawing, and heating–cooling), but its average droplet size increased during storage at different temperatures. The nanoemulsion contains a phenolic content equivalent to 736 mg gallic acid/mL. However, the antioxidant capacity of the essential oil ($IC_{50} = 0.78$ μ g/mL) was dismissed in the nanoemulsion ($IC_{50} = 2.43$ μ g/mL). The antimicrobial activity of the nanoemulsion showed strain-dependent behavior with MIC ranging from 0.0468 to 0.75 mg/mL, where *E. coli* and *S. typhimurium* were the most susceptible pathogenic bacteria. Finally, nanoencapsulation of clove oil showed higher in vitro cytotoxic activity against Caco-2 cancer cells (227 μ g/mL) than free clove essential oil (283 μ g/mL), but nanoemulsion (306 μ g/mL) was less effective than oil (231 μ g/mL) in the HT-29 line. This research shows the potential of clove essential oil nanoemulsions for developing biological therapies to treat diseases.

Keywords: droplet size; oily phase composition; surfactant–oil ratio; non–ionic surfactants; bioactivities; surface response methodology



Citation: Haro-González, J.N.; Schlienger de Alba, B.N.; Martínez-Velázquez, M.; Castillo-Herrera, G.A.; Espinosa-Andrews, H. Optimization of Clove Oil Nanoemulsions: Evaluation of Antioxidant, Antimicrobial, and Anticancer Properties. *Colloids Interfaces* **2023**, *7*, 64. <https://doi.org/10.3390/colloids7040064>

Academic Editors: Eleni P. Kalogianni, Julia Maldonado-Valderrama and Reinhard Miller

Received: 9 August 2023

Revised: 29 September 2023

Accepted: 14 October 2023

Published: 27 October 2023



Copyright: © 2023 by the authors. Licensee MDPI, Basel, Switzerland. This article is an open access article distributed under the terms and conditions of the Creative Commons Attribution (CC BY) license (<https://creativecommons.org/licenses/by/4.0/>).

1. Introduction

Syzygium aromaticum L. is an aromatic flower of the *Myrtaceae* family, cultivated in subtropical countries such as Madagascar, Sri Lanka, Indonesia, and China. *S. aromaticum* L. contains approximately 15–20% essential oil (EO), named clove essential oil (CEO). More than 30 compounds have been identified in the CEO, the proportion of which depends mainly on botanical origin and extraction method. Eugenol is the main compound of CEO (from 50% to 90%), and the complement (from 10% to 40%) is mainly composed of β -caryophyllene and α -humulene [1]. However, the volatile nature, hydrophobicity, and its impact on organoleptic properties hinder the direct use of CEO in food, cosmetic, or pharmaceutical products [2,3]. CEO has been traditionally used as an antimicrobial,

insecticide, analgesic, and anesthetic. Still, recent findings have demonstrated anticancer activity against different types of cancer, including breast, cervical, prostate, and colon cancer, with the latter being the third in terms of prevalence worldwide [1,4]. Encapsulation in emulsions, vesicles, or cyclodextrins is a common practice used to improve the compatibility and bioavailability of EOs.

An emulsion is a thermodynamically unstable colloidal dispersion formed by mixing the oil and water phases using one or more surfactants. Emulsions are usually classified by their size (nanoemulsions or macroemulsions), type of emulsifier (ionic, non-ionic, zwitterionic), formation mechanism (high energy or low energy), or external phase compatibility (W/O or O/W). If the average size is higher than 100 nm, they are referred to as macroemulsions, while if the average size is lower than 100 nm, they are called nanoemulsions (NEs). Both emulsions are kinetically metastable; however, NEs are superior in stability due to their nanometric size [5,6]. NEs are translucent or transparent in appearance, with high surface area, dispersibility, and shelf life, making them excellent systems for enhancing the solubility, bioavailability, and selectivity of bioactive compounds and essential for substance delivery, including drugs, vitamins, flavoring agents, antioxidants, polyunsaturated fatty acids, and EOs [2,3,5,7–10].

NEs can be produced by high or low-energy methods. Low-energy methods have small droplets by a delicate colloidal balance between water, oil, and surfactant or by catastrophic temperature changes. High-energy processes use specialized equipment that reduces droplet size by intense shear, high pressure, or cavitation effects, the most commonly used being high-shear microfluidizers, homogenizers, or ultrasonicator devices [2,3,11,12]. Among them, ultrasonication produces stable NEs by applying energy (approximately 10^3 – 10^5 kJ/m³), generating mechanical vibrations, and acoustic cavitation (typically 20 kHz) using a sonotrode tip. These ultrasonic waves pass through the liquid medium, inducing combined bubble nucleation, growth, and implosive collapse. The final droplet size distribution depends on several factors, such as the power supplied, the diameter of the probe, the selected amplitude, the sonication time, the volume fraction of the dispersed phase, the viscosity of the sample, and the type and concentration of the surfactant, as well as the ratio of oil-surfactant. NEs require carefully selecting variables to achieve the desired droplet size and stability, thus obtaining excellent resistance against aggregation and gravitational processes [5,11,12].

Some authors reported that sonication processors produced smaller NEs than microfluidizers [5,11]. Ibrahim et al. [13] reported smaller droplet size after 5 min of ultrasonication compared to 10 min. Additionally, the oil-surfactant ratio was observed to affect the droplet size, with a smaller droplet size obtained with an oil-surfactant ratio of 1 than 0.5. In the same vein, the surfactant plays an essential role in the formation of NEs, as Fu et al. [14] reported that the use of Tween 80 to form clove essential oil nanoemulsion (CEO-NE) was better than other surfactants such as Tween 20, Tween 40, or Tween 60. These results were like those of Nagaraju et al. [15] and Wan et al. [16], who reported that Tween 80 presented the smallest droplet size compared to other surfactants. Some reports have suggested that the polar components of the EO promote Ostwald ripening, leading to NE instability [8]. More stable NEs have been produced by partially substituting EO with medium-chain triglycerides (MCTs) or long-chain triglycerides, also called the percentage of substitution [8]. For example, Wan et al. [8] reported that substituting the EO with MTC increased the stability of NEs using a high-pressure homogenizer, reducing the droplet size from $d > 2000$ nm to 94 nm. However, the different phenolic, terpene, and alcohol content of the EOs require specific manufacturing conditions to form stable NEs [7].

Abadi et al. [12] evaluated the anticancer and cytotoxic effects of CEO-NEs on human colon cancer (HT-29) cells and their histopathological effects on the tissues of mice. In the same sense, Banerjee et al. [17] evaluated the anti-inflammatory and wound-healing potential of a CEO by emulsification with Montanov 202. Likewise, few studies have been reported that compare the bioactivity of free and encapsulated CEO, such as the one reported by Franklyne et al. [2] that evaluated the antibacterial activity of a CEO-NE

(oil:surfactant:water ratio of 2:6:92, using Tween 20 as surfactant) against five pathogens (*E. coli*, *S. enterica*, *S. paratyphi*, *S. typhimurium* and *S. boydii*), observing a reduction in the minimum inhibitory concentration and the minimum bactericidal concentration of the oil from 31–250 $\mu\text{L}/\text{mL}$ to 15–28 $\mu\text{L}/\text{mL}$ with the formation of the emulsion.

NEs could enhance biological activity through increased permeability and solubility of EOs [2,13,18]. However, the FDA points to specific concentrations as maximum daily exposure (432 mg for Tween 80), and high surfactant concentrations have been reported to produce toxic effects even after digestion [19–21]. This research aimed to develop clove essential oil nanoemulsions using the minimum concentration of surfactant and the maximum concentration of the oily phase. Different stability tests, such as centrifugation, freeze–thawing, heating–cooling, and storage temperatures, evaluated the optimal nanoemulsion. In addition, the impact of clove oil nanoencapsulation on antioxidant, antimicrobial, and anticancer activities was also investigated.

2. Materials and Methods

2.1. Materials

Clove essential oil (CEO, No. W232300), Tween 80 (T, No. P1754), 2,2-Diphenyl-1-picrylhydrazyl (DPPH, No. D9132), Folin reagent (No. F9252), Trolox (238813), Dulbecco's modified Eagle's medium (DMEM, D7777), 3-(4,5-dimethyl-2-thiazolyl)-2,5-diphenyl-2H-tetrazolium bromide (MTT, 298–93–1), and Dimethyl sulfoxide (DMSO, 276855) were obtained from Sigma–Aldrich (Toluca de Lerdo, Mexico State, Mexico). MCT oil was purchased from Gomas Naturales (Mexico City, Mexico). Absolute ethanol and methanol were purchased from “EMYR” (Jalisco, Mexico). Deionized distilled water was used in all experiments. All other reagents were analytical grade.

2.2. Methods

2.2.1. Preparation of Nanoemulsions by Ultrasonication

The NEs were prepared in two stages. First, pre-emulsions were produced by mixing the ingredients for 1 min at 13,000 rpm (T25 Ultra-Turrax, IKA Works, Inc., Wilmington, NC, USA), according to Table 1. Second, NEs were produced by sonication of an ultrasonic homogenizer of 50 W at 20 kHz (FB50, FisherBrand, Pittsburgh, PA, USA). The sonotrode probe is made of titanium with a diameter of 3 mm. Samples were kept below 30 °C using a water bath container with ice. The samples were hermetically sealed and stored at 20 °C [5,22]. The optimization of the clove essential oil nanoemulsions (CEO–NEs) was undertaken using fractional factorial 2^3 + star points, comprising 14 experiments and 5 center points (Table 1). Based on previous studies, the dispersed phase fraction [*O*], percent of substitution of CEO [*Subs*], and the percent of surfactant [*S*] were selected as the independent variables, and the *Z-ave* (nm) was the dependent variable. The design was generated and evaluated using Statgraphics Centurion XV 15.2.06 statistical software (Statgraphics Technologies, Inc., Warrenton, VA, USA), fitting a quadratic model as follows:

$$Y = \beta_0 + \sum_{i=1}^3 \beta_i x_i + \sum_{i=1}^3 \beta_{ii} x_i^2 + \sum_{i=1}^3 \sum_{j=1}^3 \beta_{ij} x_i x_j \quad (1)$$

The response was minimized based on desirability: minimizing the surfactant concentration and maximizing the percentage of substitution and oily phase in the emulsion. An analysis of variance (ANOVA) test was used to determine the differences between treatment mean values ($p < 0.05$) according to Tukey's test [5].

Table 1. Experimental design of different conditions.

Run	Experimental Run Number	Parameters			Experimental Response	Fitted Response
		% Oil Phase [O]	% Substitution Subs	% Surfactant [S]	Z-ave (nm)	Z-ave (nm)
1	19	20.0	0	1.0	366.0	394.0
2	7	2.5	0	1.0	160.2	172.4
3	1	2.5	100	4.0	255.1	228.4
4	15	2.5	100	1.0	144.8	166.9
5	14	11.3	0	2.5	245.9	167.5
6	9	2.5	50	2.5	134.9	68.3
7	18	20.0	100	1.0	697.8	640.0
8	3	11.3	50	4.0	177.8	177.2
9	4	2.5	0	4.0	130.0	189.1
10	12	11.3	50	1.0	226.0	221.6
11	5	20.0	0	4.0	264.5	243.7
12	8	20.0	50	2.5	270.6	332.1
13	16	20.0	100	4.0	545.4	534.5
14	11	11.3	100	2.5	236.9	310.2
15	17	11.3	50	2.5	151.0	158.7
16	10	11.3	50	2.5	153.9	158.7
17	13	11.3	50	2.5	157.5	158.7
18	6	11.3	50	2.5	157.4	158.7
19	2	11.3	50	2.5	163.4	158.7

2.2.2. Emulsion Droplet Size Distribution

The mean droplet size (DS) and polydispersity (PDI) index were measured using a Zetasizer Nano-ZS90 (Malvern Instruments, Malvern, UK). Each sample was diluted to approximately 0.01 g/mL with distilled water (25 °C, 0.88 cP, RI = 1.330) and placed into a glass cuvette (ZEN0118, Malvern Instruments) for measurement [5,11].

2.2.3. Stability Testing of Nanoemulsions

The stability of NEs was evaluated by employing stability tests, including centrifugation, freeze–thaw cycles, heating–cooling cycles, and storage at different temperatures [2].

Centrifugation studies: NEs were centrifuged for 30 min at 3400 × g. Those that showed no visual phase separation were considered stable to centrifugation.

Freeze–thaw cycle: NEs were kept at −20 °C for 24 h. Afterward, the NEs were maintained at 20 °C for 24 h. The cycle was repeated five times. Samples with visual phase separation were considered unstable.

Heating–cooling cycle: Five cycles of heating were used to visualize the presence of visual phase separation of the samples in the range between 4 and 40 °C with 24 h storage.

Storage temperature: The NEs were stored in different temperatures (4, 20, and 37 °C) for 35 days. NEs with visual phase separations were reported as unstable. Subsequently, the mean droplet size of the samples was measured.

2.2.4. Antioxidant Activity

DPPH Radical Capture Assay

Approximately 0.004 g of DPPH reagent was dissolved in 100 mL of ethanol. After 30 min of incubation at room temperature in the dark with the addition of 20 µL of sample and 200 µL of DPPH solution, the absorbance at $\lambda_{\max} = 595$ nm was measured. CEO was diluted in ethanol at a concentration ranging from 0.015 to 0.0955 µg/mL, while the CEO–NE was diluted at a concentration from 0.01 to 5.0 µg/mL. The concentration was determined by the concentration of free oil or the amount of oil in the NE. A Trolox

calibration curve was used in different concentrations ranging from 0.01 to 0.1 mg/mL to authenticate the process.

$$\% \text{ Scavenging} = \left[1 - \frac{\text{Abs sample}}{\text{Abs control}} \right] * 100\% \quad (2)$$

The IC_{50} values were calculated using linear regression, and the degree of scavenging was expressed as Trolox equivalent antioxidant capacity (TEAC) and calculated by the following equation [23]:

$$TEAC = \frac{IC_{50} \text{ of Trolox}}{IC_{50} \text{ of Sample}} \quad (3)$$

Determination of Total Phenol Content

CEO was dissolved in 80% ethanol (1 mL) and then diluted with distilled water in a 1:1 ratio. In each well, we added 50 μ L of diluted extract and 50 μ L of 1N Folin reagent, and we did this in triplicate. The reaction was conducted for 5 min. Then, 100 μ L of 7.5% Na_2CO_3 was added, homogenized, and incubated at room temperature for 2 h. Absorbance was determined at $\lambda_{max} = 765$ nm. Gallic acid (GA) was used as standard (0.01–0.06 mg/mL), and the total phenol content was expressed as mg GA/mL of the extract [23]. The concentration was determined by the concentration of free oil or the amount of oil in the NEs.

2.2.5. Antimicrobial Activity

Bacterial cells were cultured at 37 °C in Brain Heart Infusion (BHI) broth for the pathogenic strains (*Staphylococcus aureus*, *Listeria monocytogenes*, *Escherichia coli*, and *Salmonella typhimurium*) and in de Man, Rogosa, and Sharpe (MRS) broth for probiotic strains (*Lactiplantibacillus plantarum*, *Lactobacillus acidophilus*, and *Lacticaseibacillus rhamnosus*).

Well Diffusion Assay

Next, 100 μ L of 0.5 McFarland cell inoculum was spread on the Mueller–Hinton agar surface. A 6–8 mm diameter hole was drilled on the surface, on which 100 μ L of each treatment was placed. The plates were incubated, and by diffusion, each treatment inhibited bacterial growth. The diameter of the zone of inhibition was measured to assess its antimicrobial activity [24]. The concentration was determined by quantifying the amount of free oil and oil within the NEs.

Minimal Inhibitory Concentration (MIC)

The assay was performed using the microdilution method in 96-well plates. The following concentrations of samples were used for this assay: 0.75, 0.375, 0.1875, 0.0937, and 0.0468 mg/mL in Mueller–Hinton broth. After the growth of bacterial cells, a bacterial inoculum was standardized according to a 0.5 McFarland scale. For the assay, 20 μ L of each bacterial suspension was inoculated into 200 μ L of medium containing the concentrations of each treatment. After incubation at 37 °C for 24 h, 20 μ L of 2,3,5-triphenyltetrazolium chloride was added to the wells and incubated for 3 h. Red/pink coloration indicates bacterial growth, whereas a lack of coloration means an absence of cell growth. The concentration in which no bacterial growth was observed was taken for the MIC value [25]. The concentration was determined by quantifying the amount of free oil and oil within the NE.

Minimum Bactericidal Concentration (MCB)

MBC was determined by subculturing the dilutions at and above the MIC on agar plates and incubating at 37 °C for 24 h. The treatment concentration in which no bacterial growth was taken for the MBC value. The concentration was determined by quantifying the amount of free oil and oil within the NEs.

2.2.6. Anticancer Activity

Cell Lines and Culturing

Colorectal cancer is the third most recurrent cancer worldwide [1,4]. The anticancer activity of the CEO was measured against two different colorectal adenocarcinomas (Caco-2 and HT-29, ATCC, Rockville, MD, USA). The cells were maintained in DMEM supplemented with 10% fetal bovine serum and 1% penicillin–streptomycin–neomycin antibiotic mixture. The cultures were incubated in a wet atmosphere with 5% CO₂ and 95% air at 37 °C (Heracell™ VIOS 160i CO₂, Thermo Fisher Scientific Inc., Waltham, MA, USA) [26,27].

Cytotoxicity Assay

In vitro, cytotoxic assays were performed using the 3-(4,5-dimethyl-2-thiazolyl)-2,5-diphenyl-2H-tetrazolium bromide (MTT). Approximately 1×10^4 cells of each cell line were placed in a 96-well plate with 200 µL of culture medium. Cells were incubated for 24 h. The medium was removed, and 100 µL of the treatments (50–550 µg/mL) were added to each well. The concentration was determined by quantifying the amount of free oil and oil within the nanoemulsions (NEs). Stock treatments were dissolved in DMSO. Cells without treatments were used as negative control samples. Cells were incubated again for 24 h [24,27,28].

After incubation, 20 µL of MTT (0.5 mg/mL in PBS) was added to each well and incubated at 37 °C for 4 h. Afterward, the medium was carefully removed, and the formazan precipitates were solubilized in 100 µL DMSO. The absorbance was measured at 570 nm and reference wavelength at 690 nm using a spectrophotometer (Multiskan GO microplate, Thermo Fisher Scientific Inc., Waltham, MA, USA). The absorbance of untreated cells represented 100% cell viability. Cell viability was calculated as follows:

$$\text{Cell viability (\%)} = \frac{\text{Sample}_{abs}}{\text{Control}_{abs}} * 100\% \quad (4)$$

Dose–response viability curves determined the median inhibitory concentration (IC₅₀) for each treatment. IC₅₀ was calculated using a non–linear fit (log(inhibitor) vs. normalized response–variable slope) in GraphPad Prism 5.01 software for Windows (GraphPad Software, Inc., San Diego, CA, USA).

2.2.7. Statistical Analysis

Analyses were performed in triplicate. Data were expressed as mean ± standard deviation. One–way analysis of variance (ANOVA) was performed using Statgraphics Centurion XV 15.2.06 statistical software (StatPoint Technologies, Inc., Warrenton, VA, USA). Tukey’s test was performed to identify significant differences between treatments ($p < 0.05$).

3. Results and Discussion

3.1. Optimization of Conditions to Produce CEO–NEs

A surface response methodology was applied to evaluate the effects of oily phase [O], percent substitution [Subs], and surfactant concentration [S] on the *Z-ave* of CEO–NEs produced by ultrasonication (Table 1).

In general, the *Z-ave* of the NEs ranged from 130 to 700 nm. The coefficient of determination (R²) and the adjusted coefficient of determination (adjusted R²) of the average droplet size indicate the accuracy of the regression model. An ANOVA was performed to determine the significance of the coefficient of the quadratic polynomial equations (Table 2). A large F–value and a small *p*–value means that the means are significantly different. The coefficient of determination of the quadratic model optimized for droplet size was 0.93. These results indicate that the quadratic model is adequate for predicting the droplet size of CEO–NEs, as shown by the fitted response values in Table 1.

Table 2. ANOVA results for the droplet size of the CEO–NEs.

Variable	<i>Z-ave</i>				
	Sum of Squares	Df	Mean Square	F-Ratio	<i>p</i> -Value
Main effect					
A: [O]	174,029	1	174,029	53.28	0
B: <i>Subs</i>	50,889.2	1	50,889.2	15.58	0.0034
C: [S]	4931.36	1	4931.36	1.51	0.2503
Interaction effect					
AB	31,626.1	1	31,626.1	9.68	0.0125
AC	13,938.9	1	13,938.9	4.27	0.0688
BC	1000.54	1	1000.54	0.31	0.5934
Quadratic effect					
AA	4711.4	1	4711.4	1.44	0.2604
BB	17,578.3	1	17,578.3	5.38	0.0455
CC	4531.61	1	4531.61	1.39	0.2691
Total error	29,396.4	9	3266.27		
Total (corr.)	0.16996	18			
R-squared	0.93				
R-squared (adjusted for d.f.)	0.85				

The observed (experimental) and fitted (predicted) values for the droplet size are shown in Table 1. The analysis of variance data (Table 2) shows that [S], the [O] [S] and *Subs*[S] interactions, and the [O] and [S] quadratic terms had no significant impact among the NEs produced ($p > 0.05$). Additionally, the concentrations of [O], the [O]*Subs* interaction, and the *Subs* quadratic term significantly affected droplet size. The *Z-ave* can be calculated by the Equation (4). The [O], [O]*Subs* and *Subs*² effects increased the droplet size, while the *Subs* reduced the droplet size.

$$Z\text{-ave} = 226.73 + 3.64[\text{O}] - 3.77\text{Subs} - 76.98[\text{S}] + 0.54[\text{O}]^2 + 0.14[\text{O}]\text{Subs} - 3.18[\text{O}][\text{S}] + 0.03\text{Subs}^2 + 0.15\text{Subs}[\text{S}] + 18.10[\text{S}]^2 \quad (5)$$

These results suggest that values moderate of substitution ($20 < \text{Subs} < 85$) can produce NEs using a lower surfactant concentration [S]. The contour plot and response surface contour of the NEs *Z-ave* an elliptical boundary of the *Subs* and [O] at a [S] = 1% (Figure 1a,b). The gray-shaded region shows the conditions to produce NEs (DS < 100 nm). Based on the response surface plot for droplet size, the quadratic model predicted a significant increase in droplet size for higher [O] and low or high *Subs*. Different authors reported that the oil phases have different polarity, viscosity, interfacial tension, phase behavior, or optimal curvature of the oil phase, which can affect the formation, *Z-ave*, and characteristics of the NEs [2,8–10]. Wan et al. [8] reported that partial replacement of the oily phase with essential oil decreases the size of the NE from over 1000 nm to 94 nm when replacing 25% of the MCT oily phase with CEO.

During optimization, the desirability values were established as the minimum droplet size, the maximum percentage of the oil phase, and the percentage of substitution using the lowest surfactant concentration. The optimized formula and predicted responses are 2.5% of [O], 50.7% of *Subs*, and 1.0% of [S], and the predicted response of 89 nm. Statistical models were validated using the predicted optimal conditions shown in Table 3. The experimental *Z-ave* was 93 nm with a deviation of less than 5.0% error compared to the predicted data. This result demonstrates the high accuracy of the models used. The sizes obtained were similar to those described by Wan et al. [7], who reported the formation of an NE with an average size of 91 nm using 2.5% CEO, 2.5% MCT-oil, and 0.5% Tween 80 and 15,000 psi and three high-pressure homogenization cycles. Wan et al. [16] reported that a similar composition of 1.5% clove oil, 3.5% corn oil, and 1.0% Tween 80 using 10,000 psi

and two high-pressure homogenization cycles produced emulsions with an average size of 130 nm.

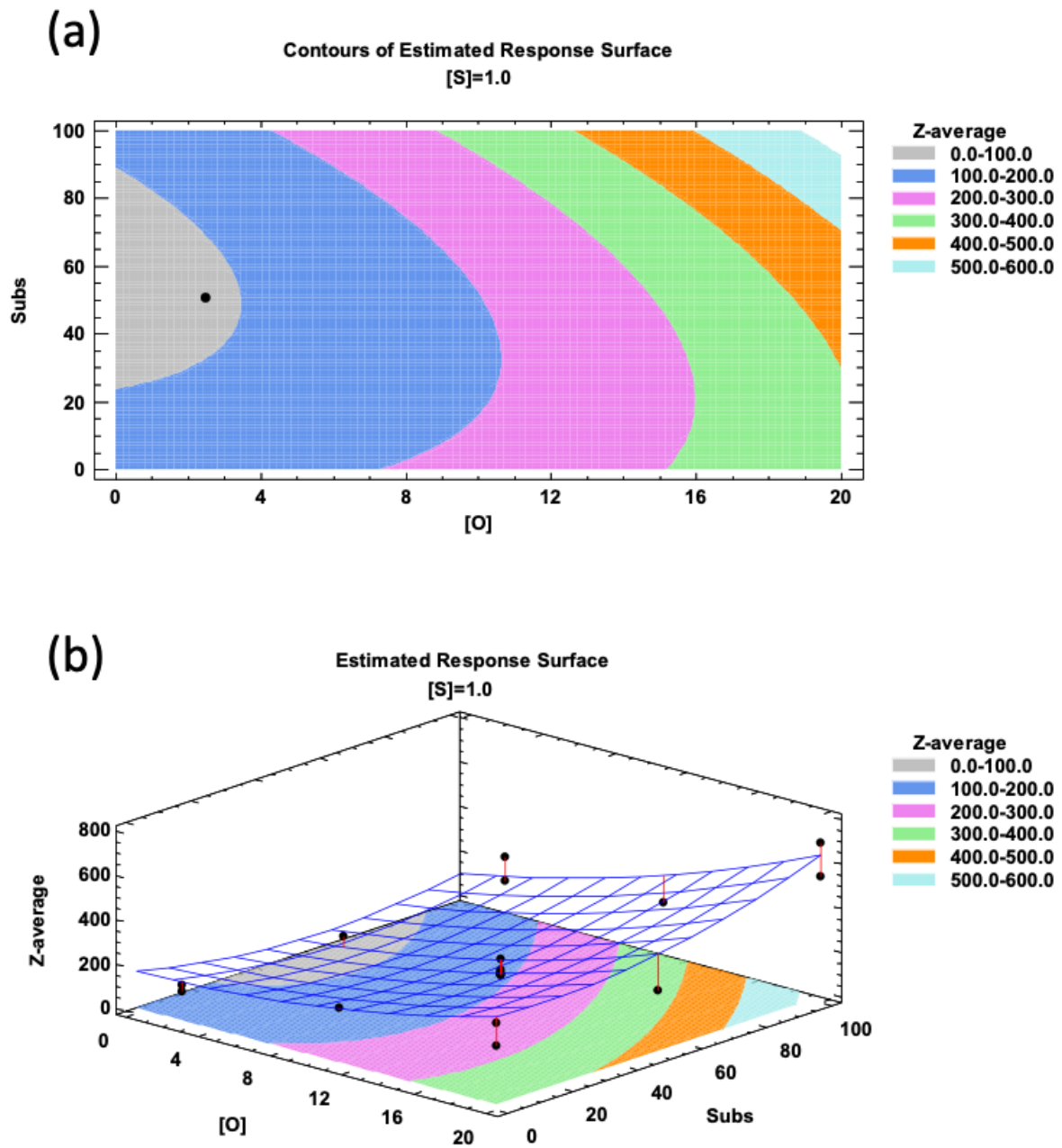


Figure 1. (a) Contour and (b) Response surface contour.

Table 3. Stability of the CEO-NE.

Test	CEO	
Centrifugation	✓	
Freeze-thaw cycle	✓	
Heating-cooling cycle	✓	
	Z-ave (nm)	PdI
Fresh	93.19 ± 3.92	0.1 ± 0.04
4 °C	146.56 ± 23.62	0.08 ± 0.05
20 °C	272.88 ± 32.97	0.13 ± 0.07
37 °C	673.90 ± 19.07	0.22 ± 0.03

3.2. Characterization and Evaluation of the Optimized Nanoemulsion

The stability of an NE ensures a long shelf life during storage. Centrifugation tests, freezing cycles, and heating cycles evaluated the stability of NEs. The purpose of the centrifugation test was to subject the NEs to centrifugal force, accelerating their instability to gravitational forces such as sedimentation or creaming. According to Restu et al. [29], subjecting NEs to 3500 rpm for 20 min is equivalent to comparable stability of one year, where a higher separation index indicates a lower percentage of stability.

A freeze–thaw cycle evaluates the effect of the formation of ice crystals during the freezing process in the optimized NE and its effect on the breakup of the droplets during thawing. The results showed that the optimized NE was stable to the freeze–thaw cycle. On the other hand, heating–cooling cycles are intended to evaluate the effect of rapid temperature changes on the stability of NEs by simulating heating or cooling processes. At higher temperatures, the viscosity of the sample decreases, increasing the collisions between the droplets and the density difference between the phases. This could weaken the interfacial film surrounding the droplets and favor destabilization. In addition, as the temperature increases, the hydration of nonionic surfactants in water decreases. The optimized CEO–NE demonstrated stability during five heating–cooling cycles. Typically, it is imperative to note that for the creation of stable O/W, NEs require a specific hydrophilic–lipophilic balance (HLB) range of 12 to 16. In this study, Tween 80 (HLB = 14.9) was used as a non–ionic surfactant. The presence of sizes less than 100 nm, a low polydispersity index, and high HLB values contributed to the generation of stable systems [2].

The storage stability of the optimized NE was evaluated after 30 days in different storage temperatures (4, 20, and 37 °C) and the *Z-ave* and PdI of the samples increased during the experimentation (Figure 2). The particle size distribution of the CEO–NEs was observed to double, quadruple, and septuple at 4, 20, and 37 °C, respectively. PdI is a metric employed to describe the droplet size distribution, i.e., narrow distributions, $PdI \leq 0.2$; broader distributions, $PdI > 0.7$. The PdI increase, however, remained low, which was reflected in a monomodal dispersion of samples [5].

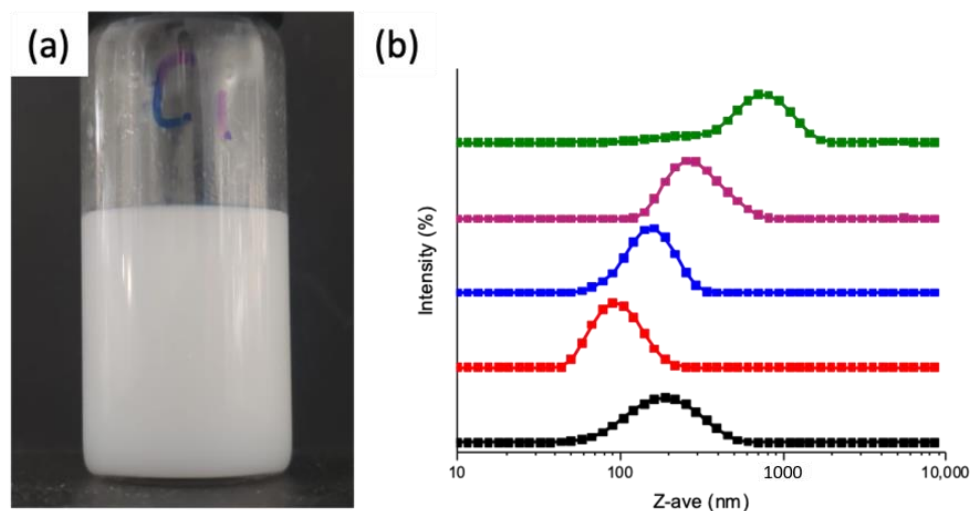


Figure 2. (a) Freshly made CEO–NE; (b) Change of the droplet size distribution after 31 days of storage at different temperatures: Control NE (black), Fresh NE (red), 4 °C (blue), 20 °C (purple), and 37 °C (green).

The storage of NEs at high temperatures reduces the interfacial tension, which increases the flexibility of the surfactant layer and makes it more susceptible to destabilization. The properties of non–ionic surfactants are determined by their hydrophilic–lipophilic balance (HLB), which is temperature–dependent. Elevated temperatures increase the hydrophobic character and reduce the solubility of the surfactant, resulting in increased hydrophobicity and cloudiness as the temperature rises. Clouding occurs because the

water molecules bonded to the ether oxygen of the polyoxyethylene group of non-ionic surfactants are detached [30]. Chang et al. [9,10] reported that low concentrations of EOs decrease the coalescence processes due to the polarity and low interfacial tension of EOs. Similar results were reported by Wan et al. [8], a slight increase in NE droplet size was observed using a high-pressure homogenizer (15,000 psi and three passes) with 1.25% CEO during 30 days of storage at 4 and 25 °C.

Wan et al. [7] observed that the diameter of high-pressure NEs (2.5% CEO) remained constant during 30 days of storage, inhibiting the Ostwald ripening process. Franklyne et al. [2] reported stability greater than 4 months for an NE by ultrasonication ($d < 24$ nm, 20 min at 40% intensity) with a six times higher concentration of surfactant (Tween 20) and 2% CEO. They also reported that controlling the oil:surfactant:water ratio is necessary to obtain stable NEs. Ibrahim et al. [13] reported an increase in the size of NEs produced by ultrasonication after 60 days of storage. The size doubled and quadrupled with 5% and 10% eugenol concentration, respectively. Wan et al. [16] reported that the diameter of NEs (1.5% clove oil, 3.5% corn oil, and 1.0% Tween 80) tripled (from 130.95 nm to 406.33 nm) after 7 days of storage. The high long-term instability could be due to the Oswald maturation phenomenon, in which the increase in particle size is favored by the oil migration from small to larger droplets. The presence of Tween 80 at a concentration higher than its critical micellar concentration allowed the formation of micelles, which were able to solubilize and transport the clove oil molecules in the aqueous phase into its hydrophobic interior [16].

3.3. Antioxidant Activity

Phenolic compounds in EOs are known for their ability to donate hydrogen to radicals, which is closely linked to their antioxidant properties. The Trolox IC_{50} was 76.02 ± 4.24 $\mu\text{g}/\text{mL}$. The TPC and antioxidant activity of the CEO and the CEO-NE are presented in Table 4.

Table 4. Antioxidant activity of the nanoemulsions.

	IC_{50} (μg CEO/mL)	TEAC	TPC (mg of GA/mL)
CEO	0.78 ± 0.04^a	97.95 ± 9.91^a	683.13 ± 77.85^a
CEO-NE	2.43 ± 0.07^b	31.30 ± 1.7^b	736.04 ± 13.94^a

DPPH; IC_{50} : half maximal inhibitory concentration; TEAC: Trolox equivalent antioxidant capacity; TPC: Total phenolic content. Different letters in the same column represent the significance between treatments.

The antioxidant activity of CEO was evaluated by measuring their ability to donate hydrogen or scavenge radicals, resulting in the conversion of DPPH• to non-radical DPPH-H. CEO showed an IC_{50} value of 0.78 $\mu\text{g}/\text{mL}$. The optimized CEO-NE contains a CEO concentration of 1.25 mg/mL with an IC_{50} value of 2.43 μg CEO/mL, corresponding to 194 μg per mL of NE. Ivanovic et al. [31] reported an IC_{50} of 20.64 $\mu\text{g}/\text{mL}$ for an extract obtained by supercritical fluid containing 68% eugenol. Ramadan et al. [26] found that CEO, rich in eugenol (82%), had superior antioxidant activity compared to the synthetic antioxidant TBHQ EOs of thyme and juniper. CEO has been reported to have higher radical scavenging activity compared to 26 other essential oils, including jasmine, chamomile, thyme, cardamom, eucalyptus, black fir, cinnamon, nutmeg, basil, oregano, and thyme [32].

Several factors can impact the antioxidant capacity of emulsions, such as the type and concentration of the oil phase and surfactant, pH and ionic composition, emulsion size, and interfacial properties, as well as the location of antioxidants in the oil phase and polarity. However, better protection is reported in emulsions with a high surfactant content [33–35]. Almajano et al. [35] reported that the antioxidant activity of emulsions depends on the type of catechin and protein incorporation. This dependence on encapsulation was also reported by Kiralan et al. [34], who evaluated the physical location of the antioxidants (α , γ , and δ tocopherols) at the interface and the concentration of the surfactant (Tween 20, 0.1%, 0.5%, and 1%). They reported that the antioxidant activity not only depends on the increase in the concentration of the surfactant but also the polarity of the tocopherols, which is

greater in α -tocopherol (three methyl groups) than in δ -tocopherol (one methyl group). One objective of our study was to reduce the concentration of the surfactant, which may be reflected in the decrease in antioxidant activity.

Phenolic compounds are widely recognized for their beneficial health effects, as they exhibit diverse biological activities. CEO contains phytochemicals with varied chemical structures, which could be responsible for the different pharmacological and biological activities [1]. In this sense, Ivanovic et al. [31] reported that the clove extract obtained by supercritical fluid (68% eugenol) had a TPC of 530.56 mg GAE/g. CEO has been reported to have a higher TPC compared to other essential oils, such as thyme borneol, chamomile, ylang ylang, jasmine absolute, bourbon vetiver, petitgrain bigarade, and rosewood essential oil [32].

3.4. Antimicrobial Activity

The antibacterial activities of CEO and NE against four pathogenic bacteria (*S. aureus*, *L. monocytogenes*, *E. coli*, and *S. typhimurium*) and three probiotic strains (*Lpb. Plantarum*, *Lb. acidophilus*, and *Lcb. rhamnosus*) are shown in Table 5.

The pathogenic bacteria were selected for their importance at a clinical level since they are the main cause of infections in tissues and other systems, such as the gastrointestinal system. Furthermore, it was essential to examine how the nanoemulsion and the oil affected probiotic bacteria, which are beneficial microorganisms for human well-being. Well diffusion agar assay verified that all treatments exhibited a strong antibacterial effect against all pathogenic bacterial strains, while no effect was observed against probiotic strains.

The results revealed that *E. coli* was more susceptible than the other bacterial strains tested in all treatments. The diameter of the zone of maximum inhibition was 13.33 mm and 17.67 mm for the CEO and CEO-NE, respectively. However, the nanoencapsulation of the CEO only showed a significantly greater effect on this strain. The antimicrobial activity of CEO is attributed to eugenol, β -Caryophyllene, and α -humulene [1]. The enhanced antimicrobial activity of NE against *E. coli* is attributed to their capacity to merge with the lipid membrane, leading to the destabilization of membrane permeability and function, ultimately resulting in cell lysis and subsequent cell death [24].

A higher diameter of inhibition was found for *E. coli* with CEO-NEs. A similar result was found for eugenol NEs [14]. This behavior was related to increased cell membrane permeability caused by the surfactant, allowing a greater internalization of the active compounds [14,36]. It is important to note that the action of the oil will depend on the bacterial strain and whether it presents any resistance mechanism, as this may reduce the antibacterial effect of the oil. For instance, eugenol oil tested with tetracycline and cefotaxime-resistant *S. aureus* had no significant impact, but in combination with each antibiotic, eugenol had a synergistic effect that reduced the MIC of both tetracycline and cefotaxime [37,38]. Also, Hu et al. [36] reported that CEO had the lowest antibacterial activity due to the lower quantity of antibacterial compounds. Another study found similar results, in which CEO inhibited both Gram-positive and Gram-negative bacteria, showing inhibition zones of 13.7–17.3 mm and 11.7–20.7 mm, respectively [39].

Table 5. In vitro antibacterial activity against some bacteria.

Microbial Strains	Sample	<i>S. aureus</i>	<i>L. monocytogenes</i>	<i>E. coli</i>	<i>S. typhimurium</i>	<i>Lpb. plantarum</i>	<i>Lb. acidophilus</i>	<i>Lcb. rhamnosus</i>
Well diffusion agar (mm)	CEO-NE	10.33 ± 0.58 ^{aA}	10.83 ± 0.76 ^{aA}	17.67 ± 0.58 ^{bB}	11.33 ± 0.29 ^{aA}	ND	ND	ND
	Clove oil	11.50 ± 0.50 ^{aAB}	11.00 ± 0.50 ^{aA}	12.33 ± 0.58 ^{aB}	11.17 ± 0.29 ^{aA}	ND	ND	ND
MIC (mg/mL)	CEO-NE	0.75	0.75	0.375	0.1875	0.1875	0.1875	0.375
	Clove oil	0.375	0.375	0.1875	0.0937	0.0468	0.0468	0.0468
MBC (mg/mL)	CEO-NE	0.75	0.75	0.375	0.375	0.75	0.75	0.75
	Clove oil	0.375	0.75	0.1875	0.1875	0.375	0.75	0.0468

The NE without CEO did not present antibacterial activity. ND: Not Determined. The lower-case letters in the same column represent significant differences between treatments, while the upper-case letters in the same row represent significant differences between bacterial cells.

To reinforce the findings, MIC and MBC were determined. MIC is defined as the lowest concentration required to inhibit visible microbial growth [25]. It was observed that the MIC values were lower for *E. coli* and *S. typhimurium* (0.187 mg/mL of CEO) than for *S. aureus* and *L. monocytogenes* (0.375–0.75 mg/mL). In a study conducted by Radünz et al. [40], they showed an inhibitory effect of clove oil with a concentration of 0.304 mg/mL against *S. aureus*, *E. coli*, *L. monocytogenes*, and *S. typhimurium*. Also, Radünz et al. [40] found a reduction in the antimicrobial capacity of CEO encapsulated with lipids such as glycerol monostearate and polyoxyethylene sorbitan monolaurate due to low interaction with the cell membrane of the bacteria. The findings suggest that the nanoemulsions did not release all the contained clove oil, which elevated the concentration required to exert the inhibitory and bactericidal action. Moreover, discrepancies in antimicrobial effectiveness against Gram-positive and Gram-negative bacteria could be attributed to porins on the outer membrane, which facilitates the passage of certain compounds based on their size [41].

The probiotic strains had the lowest MIC between 0.0468 and 0.375 mg/mL. Nevertheless, the MBC was higher than the MIC—the opposite of the pathogenic bacteria observed. Some authors point out that clove oil has a strain-dependent antimicrobial effect, such as with *Lcb. rhamnosus*, *B. animalis* subsp. *lactis* Bb-12, *B. bifidum* 89, and *B. infantis*, as was found in this study. The CEO-NE may exert a bacteriostatic action; therefore, the bactericidal concentration is greater than the inhibitory one. On the other hand, Song et al. [42] found that concentrations of eugenol lower than 1050.88 mg/mL had no antimicrobial effect on *L. plantarum* ZS2058, and when combined, a higher antimicrobial effect on *S. typhimurium* was observed.

3.5. Anticancer Activity

The antiproliferative effect of the CEO-NE and CEO was evaluated using the MTT assay. The results of the MTT assay are shown in Figure 3, where CEO-NEs have been found to act as anticancer agents on colon cancer cells.

CEO-NE showed greater anticancer activity than free CEO, but only for the Caco-2 cell line. No significant differences were observed for the HT-29 cell line. NE did not show an anticancer effect below 200 µg/mL for the HT-29 cell line but had a cytotoxic effect at concentrations above 100 µg/mL for Caco-2. In comparison, CEO had a cytotoxic effect after 200 and 300 µg/mL for Caco-2 and HT-29, respectively.

Table 6 shows the IC₅₀ values for the cancer cells obtained for CEO-NE and CEO. The MTT assay revealed a decrease in IC₅₀ due to the action of NE compared to the CEO. A complex mixture of mono and sesquiterpenes, especially eugenol, is mainly attributed to the anticancer activity of free CEO. Several reports have demonstrated the excellent dose-dependent anticancer action of essential oils against different human cancer cells, including HepG2, MCF-7, PC3, HCT116, and A549 [26,28].

Table 6. Anticancer IC₅₀ values (µg/mL) for CEO-NE and CEO.

	HT-29	Caco-2
Control	438.7 ± 71.6 ^{Aa}	538.5 ± 32.5 ^{Cb}
CEO	231.0 ± 13.8 ^{Ba}	283.3 ± 9.3 ^{Bb}
NECEO	306.6 ± 24.1 ^{Ab}	227.2 ± 5.2 ^{Aa}

Capital letters represent the significant difference between treatments, while lower-case letters represent the difference between cell lines.

The sensitivity of the HT-29 cells occurred in the following order: CEO > NE_{CEO}, while for the Caco-2 cells, it was: NE_{CEO} > CEO. The IC₅₀ of CEO obtained was higher than that reported by Nagaraju et al. [15] for Caco-2, showing a 200 µg/mL concentration. The obtained cytotoxic activity of CEO-NEs was lower than that reported by ultrasonication (74.8 µg/mL) against HT-29 and Caco-2 (200 µg/mL) [12,15].

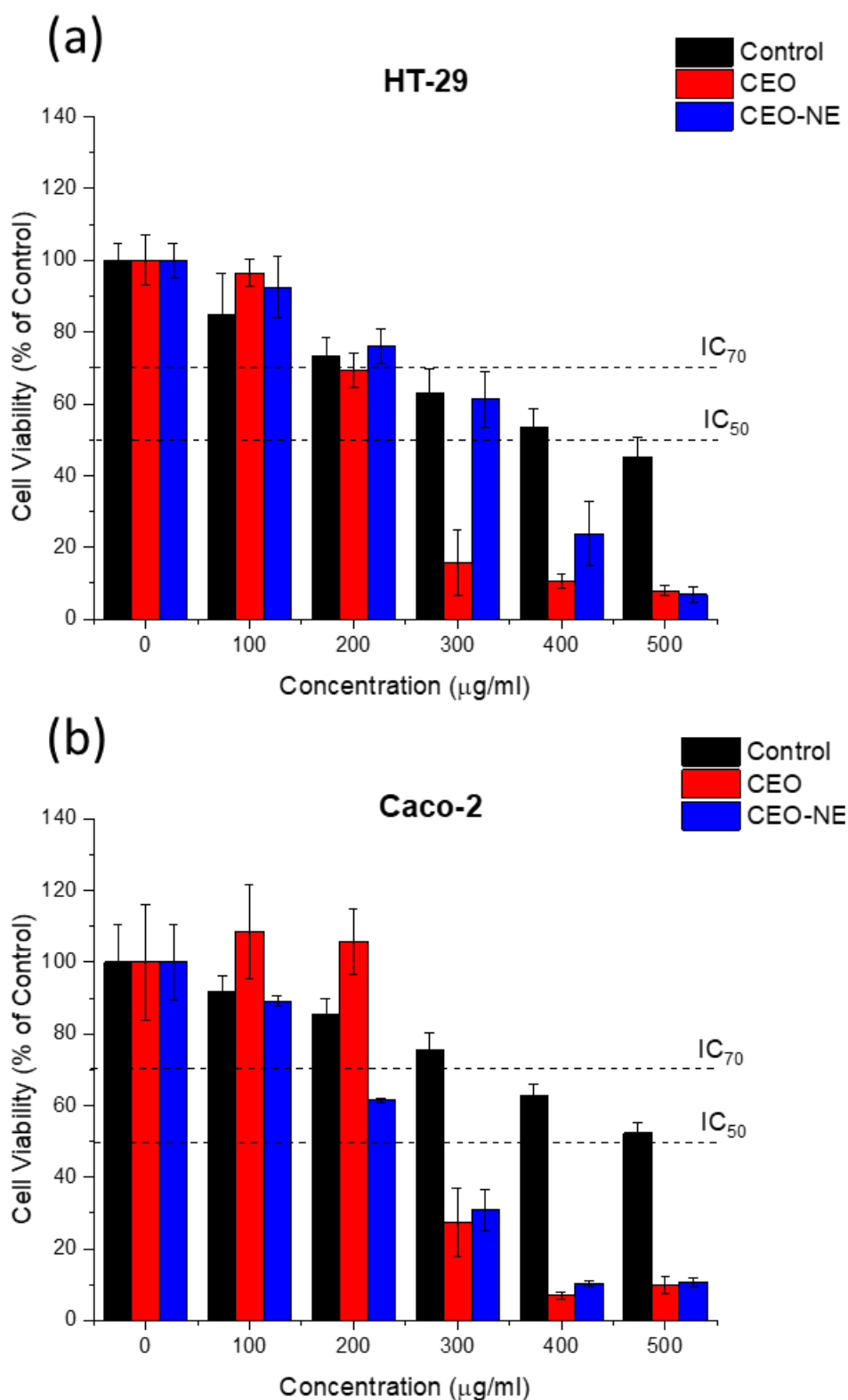


Figure 3. Effect of treatment on cell viability of (a) HT-2 and (b) Caco-2 cells after 24 h of incubation by MTT assay.

Different authors have reported that the permeability of HT-29 cells is lower compared to cell lines such as Caco-2 and HT29-MTX due to mucin production. Likewise, greater resistance has been observed in the HT-29 cells against docetaxel, oxaliplatin, 5-fluorouracil,

and camptothecin compared to other colon cancer cells, due to its higher cell proliferation and growth rate, as well as to the expression of markers related to chemoresistance [43–45].

CEO has been reported to possess anticancer activity due to its antioxidant, antimetastatic, cytotoxic, cell-cycle-regulating, apoptosis, and necrosis-inducing capacity [1,12,17,24]. The anticancer activity of CEO is related to the eugenol concentration, but also to low-concentration components such as β -caryophyllene or α -humulene [1,3,26,27]. Several authors reported that NEs enhance the anticancer activity of bioactive compounds compared to the free form (non-encapsulated). NEs enhance the solubility, penetration, absorption, and bioavailability of essential oils, as well as protect against oxidation and hydrolysis, which facilitates the induction of cell death.

4. Conclusions

Clove essential oil nanoemulsion was obtained using ultrasonic technology. The results showed that the percentage of the oil phase and the percentage of replacement of the clove essential oil significantly reduced the droplet size of the nanoemulsions low in surfactant concentration. A second-order polynomial model correctly predicted the droplet size of the nanoemulsions, generating stable nanoemulsions under accelerated stress, but with changes during long-term storage at elevated temperatures. The nanoemulsion maintained the phenolic content, but the antioxidant capacity decreased in comparison to the free essential oil. However, the antimicrobial activities were preserved in the optimized nanoemulsion. The MIC and MBC serve as foundations for establishing precise nanoemulsion dosage recommendations to optimize therapeutic benefits while minimizing risks of antimicrobial resistance and adverse effects. The anticancer activity depends on the cell line evaluated, with the Caco-2 line being more sensitive than HT-29. These results provide helpful information for developing clove essential oil nanoemulsions for nutraceutical foods.

Author Contributions: J.N.H.-G.: Conceptualization, Methodology, Formal analysis, Investigation, Writing—original draft. B.N.S.d.A.: Experiment and Methodology, Writing—original draft. M.M.-V.: Conceptualization, Validation. G.A.C.-H.: Resources, Investigation, Supervision. H.E.-A.: Conceptualization, Supervision, Writing—review and editing, Validation. All authors have read and agreed to the published version of the manuscript.

Funding: This work was supported by the SE—CONACYT CB2017-2018 [grant number A1-S-51264].

Data Availability Statement: The data presented in this study are available on request from the corresponding author.

Acknowledgments: The first author is grateful to the Consejo Nacional de Ciencia y Tecnología for the scholarship granted to study for a doctorate in science in biotechnological innovation (CVU: 844169). The second author is grateful to the Consejo Nacional de Ciencia y Tecnología for the scholarship granted to study for a doctorate in science in biotechnological innovation (CVU: 1173918).

Conflicts of Interest: The authors declare that they have no conflict of interest.

References

1. Haro-González, J.N.; Castillo-Herrera, G.A.; Martínez-Velázquez, M.; Espinosa-Andrews, H. Clove Essential Oil (*Syzygium aromaticum* L. Myrtaceae): Extraction, Chemical Composition, Food Applications, and Essential Bioactivity for Human Health. *Molecules* **2021**, *26*, 6387. [\[CrossRef\]](#)
2. Franklyne, J.S.; Iyer, S.; Ebenazer, A.; Mukherjee, A.; Chandrasekaran, N. Essential Oil Nanoemulsions: Antibacterial Activity in Contaminated Fruit Juices. *Int. J. Food Sci. Technol.* **2019**, *54*, 2802–2810. [\[CrossRef\]](#)
3. Badr, M.M.; Badawy, M.E.I.; Taktak, N.E.M. Characterization, Antimicrobial Activity, and Antioxidant Activity of the Nanoemulsions of Lavandula Spica Essential Oil and Its Main Monoterpenes. *J. Drug Deliv. Sci. Technol.* **2021**, *65*, 102732. [\[CrossRef\]](#)
4. Sung, H.; Ferlay, J.; Siegel, R.L.; Laversanne, M.; Soerjomataram, I.; Jemal, A.; Bray, F. Global Cancer Statistics 2020: GLOBOCAN Estimates of Incidence and Mortality Worldwide for 36 Cancers in 185 Countries. *CA Cancer J. Clin.* **2021**, *71*, 209–249. [\[CrossRef\]](#)
5. Espinosa-Andrews, H.; Páez-Hernández, G. Optimization of Ultrasonication Curcumin-Hydroxylated Lecithin Nanoemulsions Using Response Surface Methodology. *J. Food Sci. Technol.* **2020**, *57*, 549–556. [\[CrossRef\]](#) [\[PubMed\]](#)
6. Gupta, C.; Chawla, P.; Arora, S. Development and Evaluation of Iron Microencapsules for Milk Fortification. *CyTA-J. Food* **2015**, *13*, 116–123. [\[CrossRef\]](#)

7. Wan, J.; Zhong, S.; Schwarz, P.; Chen, B.; Rao, J. Physical Properties, Antifungal and Mycotoxin Inhibitory Activities of Five Essential Oil Nanoemulsions: Impact of Oil Compositions and Processing Parameters. *Food Chem.* **2019**, *291*, 199–206. [[CrossRef](#)] [[PubMed](#)]
8. Wan, J.; Zhong, S.; Schwarz, P.; Chen, B.; Rao, J. Influence of Oil Phase Composition on the Antifungal and Mycotoxin Inhibitory Activity of Clove Oil Nanoemulsions. *Food Funct.* **2018**, *9*, 2872–2882. [[CrossRef](#)]
9. Chang, Y.; McLandsborough, L.; McClements, D.J. Physicochemical Properties and Antimicrobial Efficacy of Carvacrol Nanoemulsions Formed by Spontaneous Emulsification. *J. Agric. Food Chem.* **2013**, *61*, 8906–8913. [[CrossRef](#)]
10. Chang, Y.; McClements, D.J. Optimization of Orange Oil Nanoemulsion Formation by Isothermal Low-Energy Methods: Influence of the Oil Phase, Surfactant, and Temperature. *J. Agric. Food Chem.* **2014**, *62*, 2306–2312. [[CrossRef](#)]
11. Páez-Hernández, G.; Mondragón-Cortez, P.; Espinosa-Andrews, H. Developing Curcumin Nanoemulsions by High-Intensity Methods: Impact of Ultrasonication and Microfluidization Parameters. *LWT* **2019**, *111*, 291–300. [[CrossRef](#)]
12. Abadi, A.V.M.; Karimi, E.; Oskoueian, E.; Mohammad, G.R.K.S.; Shafaei, N. Chemical Investigation and Screening of Anti-Cancer Potential of *Syzygium aromaticum* L. Bud (Clove) Essential Oil Nanoemulsion. *3 Biotech* **2022**, *12*, 49. [[CrossRef](#)] [[PubMed](#)]
13. Ibrahim, S.S.; Sahu, U.; Karthik, P.; Vendan, S.E. Eugenol Nanoemulsion as Bio-Fumigant: Enhanced Insecticidal Activity against the Rice Weevil, *Sitophilus Oryzae* Adults. *J. Food Sci. Technol.* **2023**, *60*, 1435–1445. [[CrossRef](#)] [[PubMed](#)]
14. Fu, X.; Gao, Y.; Yan, W.; Zhang, Z.; Sarker, S.; Yin, Y.; Liu, Q.; Feng, J.; Chen, J. Preparation of Eugenol Nanoemulsions for Antibacterial Activities. *RSC Adv.* **2022**, *12*, 3180–3190. [[CrossRef](#)] [[PubMed](#)]
15. Nagaraju, P.G.; Sengupta, P.; Chicgovinda, P.P.; Rao, P.J. Nanoencapsulation of Clove Oil and Study of Physicochemical Properties, Cytotoxic, Hemolytic, and Antioxidant Activities. *J. Food Process Eng.* **2021**, *44*, e13645. [[CrossRef](#)]
16. Wan, J.; Jin, Z.; Zhong, S.; Schwarz, P.; Chen, B.; Rao, J. Clove Oil-in-Water Nanoemulsion: Mitigates Growth of *Fusarium Graminearum* and Trichothecene Mycotoxin Production during the Malting of *Fusarium* Infected Barley. *Food Chem.* **2020**, *312*, 126120. [[CrossRef](#)]
17. Banerjee, K.; Madhyastha, H.; Rajendra Sandur, V.; Manikandanath, N.T.; Thiagarajan, N.; Thiagarajan, P. Anti-Inflammatory and Wound Healing Potential of a Clove Oil Emulsion. *Colloids Surf. B Biointerfaces* **2020**, *193*, 111102. [[CrossRef](#)] [[PubMed](#)]
18. da Silva Gündel, S.; Velho, M.C.; Diefenthaler, M.K.; Favarin, F.R.; Copetti, P.M.; de Oliveira Fogaça, A.; Klein, B.; Wagner, R.; Gündel, A.; Sagrillo, M.R.; et al. Basil Oil-Nanoemulsions: Development, Cytotoxicity and Evaluation of Antioxidant and Antimicrobial Potential. *J. Drug Deliv. Sci. Technol.* **2018**, *46*, 378–383. [[CrossRef](#)]
19. Sun, H.; Yang, R.; Wang, J.; Yang, X.; Tu, J.; Xie, L.; Li, C.; Lao, Q.; Sun, C. Component-Based Biocompatibility and Safety Evaluation of Polysorbate 80. *RSC Adv.* **2017**, *7*, 15127–15138. [[CrossRef](#)]
20. Bu, P.; Ji, Y.; Narayanan, S.; Dalrymple, D.; Cheng, X.; Serajuddin, A.T.M. Assessment of Cell Viability and Permeation Enhancement in Presence of Lipid-Based Self-Emulsifying Drug Delivery Systems Using Caco-2 Cell Model: Polysorbate 80 as the Surfactant. *Eur. J. Pharm. Sci.* **2017**, *99*, 350–360. [[CrossRef](#)]
21. Desai, H.H.; Bu, P.; Shah, A.V.; Cheng, X.; Serajuddin, A.T.M. Evaluation of Cytotoxicity of Self-Emulsifying Formulations Containing Long-Chain Lipids Using Caco-2 Cell Model: Superior Safety Profile Compared to Medium-Chain Lipids. *J. Pharm. Sci.* **2020**, *109*, 1752–1764. [[CrossRef](#)]
22. Shahavi, M.H.; Hosseini, M.; Jahanshahi, M.; Meyer, R.L.; Darzi, G.N. Clove Oil Nanoemulsion as an Effective Antibacterial Agent: Taguchi Optimization Method. *Desalination Water Treat.* **2016**, *57*, 18379–18390. [[CrossRef](#)]
23. Behbahani, B.A.; Noshad, M.; Falah, F. Study of Chemical Structure, Antimicrobial, Cytotoxic and Mechanism of Action of *Syzygium Aromaticum* Essential Oil on Foodborne Pathogens. *Potravin. Slovak J. Food Sci.* **2019**, *13*, 875–883. [[CrossRef](#)]
24. Nirmala, M.J.; Durai, L.; Gopakumar, V.; Nagarajan, R. Anticancer and Antibacterial Effects of a Clove Bud Essential Oil-Based Nanoscale Emulsion System. *Int. J. Nanomed.* **2019**, *14*, 6439–6450. [[CrossRef](#)] [[PubMed](#)]
25. Moritz, C.M.F.; Rall, V.L.M.; Saeki, M.J.; Fernandes Júnior, A. Inhibitory Effect of Essential Oils against *Lactobacillus Rhamnosus* and Starter Culture in Fermented Milk during Its Shelf-Life Period. *Braz. J. Microbiol.* **2012**, *43*, 1147–1156. [[CrossRef](#)]
26. Ramadan, M.M.; Ali, M.M.; Ghanem, K.Z.; El-Ghorabe, A.H. Essential Oils from Egyptian Aromatic Plants as Antioxidant and Novel Anticancer Agents in Human Cancer Cell Lines. *Grasas Y Aceites* **2015**, *66*, e080. [[CrossRef](#)]
27. Najar, B.; Shortrede, J.E.; Pistelli, L.; Buhagiar, J. Chemical Composition and in Vitro Cytotoxic Screening of Sixteen Commercial Essential Oils on Five Cancer Cell Lines. *Chem. Biodivers.* **2020**, *17*, e1900478. [[CrossRef](#)]
28. Kouidhi, B.; Zmantar, T.; Bakhrouf, A. Anticariogenic and Cytotoxic Activity of Clove Essential Oil (*Eugenia Caryophyllata*) against a Large Number of Oral Pathogens. *Ann. Microbiol.* **2010**, *60*, 599–604. [[CrossRef](#)]
29. Restu, W.K.; Sampora, Y.; Meliana, Y.; Haryono, A. Effect of Accelerated Stability Test on Characteristics of Emulsion Systems with Chitosan as a Stabilizer. *Procedia Chem.* **2015**, *16*, 171–176. [[CrossRef](#)]
30. Gulotta, A.; Saberi, A.H.; Nicoli, M.C.; McClements, D.J. Nanoemulsion-Based Delivery Systems for Polyunsaturated (ω -3) Oils: Formation Using a Spontaneous Emulsification Method. *J. Agric. Food Chem.* **2014**, *62*, 1720–1725. [[CrossRef](#)] [[PubMed](#)]
31. Ivanovic, J.; Dimitrijevic-Brankovic, S.; Mistic, D.; Ristic, M.; Zizovic, I. Evaluation and Improvement of Antioxidant and Antibacterial Activities of Supercritical Extracts from Clove Buds. *J. Funct. Foods* **2013**, *5*, 416–423. [[CrossRef](#)]
32. Wang, H.F.; Yih, K.H.; Yang, C.H.; Huang, K.F. Anti-Oxidant Activity and Major Chemical Component Analyses of Twenty-Six Commercially Available Essential Oils. *J. Food Drug Anal.* **2017**, *25*, 881–889. [[CrossRef](#)] [[PubMed](#)]
33. Kiokias, S.; Oreopoulou, V. Review on the Antioxidant Activity of Phenolics in o/w Emulsions along with the Impact of a Few Important Factors on Their Interfacial Behaviour. *Colloids Interfaces* **2022**, *6*, 79. [[CrossRef](#)]

34. Kiralan, S.S.; Doğu-Baykut, E.; Kittipongpittaya, K.; McClements, D.J.; Decker, E.A. Increased Antioxidant Efficacy of Tocopherols by Surfactant Solubilization in Oil-in-Water Emulsions. *J. Agric. Food Chem.* **2014**, *62*, 10561–10566. [[CrossRef](#)] [[PubMed](#)]
35. Almajano, M.P.; Delgado, M.E.; Gordon, M.H. Albumin Causes a Synergistic Increase in the Antioxidant Activity of Green Tea Catechins in Oil-in-Water Emulsions. *Food Chem.* **2007**, *102*, 1375–1382. [[CrossRef](#)]
36. Hu, J.; Zhu, H.; Feng, Y.; Yu, M.; Xu, Y.; Zhao, Y.; Zheng, B.; Lin, J.; Miao, W.; Zhou, R.; et al. Emulsions Containing Composite (Clove, Oregano, and Cinnamon) Essential Oils: Phase Inversion Preparation, Physicochemical Properties and Antibacterial Mechanism. *Food Chem.* **2023**, *421*, 136201. [[CrossRef](#)] [[PubMed](#)]
37. Bezerra, S.R.; Bezerra, A.H.; de Sousa Silveira, Z.; Macedo, N.S.; dos Santos Barbosa, C.R.; Muniz, D.F.; Sampaio dos Santos, J.F.; Melo Coutinho, H.D.; Bezerra da Cunha, F.A. Antibacterial Activity of Eugenol on the IS-58 Strain of Staphylococcus Aureus Resistant to Tetracycline and Toxicity in Drosophila Melanogaster. *Microb. Pathog.* **2022**, *164*, 105456. [[CrossRef](#)]
38. Lady, J.; Nurcahyanti, A.D.R.; Tjoa, E. Synergistic Effect and Time-Kill Evaluation of Eugenol Combined with Cefotaxime Against Staphylococcus Aureus. *Curr. Microbiol.* **2023**, *80*, 244. [[CrossRef](#)]
39. Al-Zereini, W.A.; Al-Trawneh, I.N.; Al-Qudah, M.A.; Tumallah, H.M.; Abudayeh, Z.H.; Hijazin, T. Antibacterial, Antioxidant, and Cytotoxic Activities of *Syzygium aromaticum* (L.) Merr. & Perry Essential Oil with Identification of Its Chemical Constituents. *Z. Fur Naturforschung-Sect. C J. Biosci.* **2023**, *78*, 105–112. [[CrossRef](#)]
40. Radünz, M.; da Trindade, M.L.M.; Camargo, T.M.; Radünz, A.L.; Borges, C.D.; Gandra, E.A.; Helbig, E. Antimicrobial and Antioxidant Activity of Unencapsulated and Encapsulated Clove (*Syzygium aromaticum*, L.) Essential Oil. *Food Chem.* **2019**, *276*, 180–186. [[CrossRef](#)]
41. Falleh, H.; Ben Jemaa, M.; Neves, M.A.; Isoda, H.; Nakajima, M.; Ksouri, R. Formulation, Physicochemical Characterization, and Anti- E. Coli Activity of Food-Grade Nanoemulsions Incorporating Clove, Cinnamon, and Lavender Essential Oils. *Food Chem.* **2021**, *359*, 129963. [[CrossRef](#)] [[PubMed](#)]
42. Song, F.; Liu, J.; Zhao, W.; Huang, H.; Hu, D.; Chen, H.; Zhang, H.; Chen, W.; Gu, Z. Synergistic Effect of Eugenol and Probiotic Lactobacillus Plantarum Zs2058 against Salmonella Infection in C57bl/6 Mice. *Nutrients* **2020**, *12*, 1611. [[CrossRef](#)] [[PubMed](#)]
43. Gagnon, M.; Zihler Berner, A.; Chervet, N.; Chassard, C.; Lacroix, C. Comparison of the Caco-2, HT-29 and the Mucus-Secreting HT29-MTX Intestinal Cell Models to Investigate Salmonella Adhesion and Invasion. *J. Microbiol. Methods* **2013**, *94*, 274–279. [[CrossRef](#)]
44. El Khoury, F.; Corcos, L.; Durand, S.; Simon, B.; Le Jossic-Corcos, C. Acquisition of Anticancer Drug Resistance Is Partially Associated with Cancer Stemness in Human Colon Cancer Cells. *Int. J. Oncol.* **2016**, *49*, 2558–2568. [[CrossRef](#)] [[PubMed](#)]
45. Verhoeckx, K.; Cotter, P.; López-Expósito, I.; Kleiveland, C.; Lea, T.; Mackie, A.; Requena, T.; Swiatecka, D.; Wichers, H. *The Impact of Food Bioactives on Health: In Vitro and Ex Vivo Models*; Springer International Publishing: Cham, Switzerland, 2015.

Disclaimer/Publisher’s Note: The statements, opinions and data contained in all publications are solely those of the individual author(s) and contributor(s) and not of MDPI and/or the editor(s). MDPI and/or the editor(s) disclaim responsibility for any injury to people or property resulting from any ideas, methods, instructions or products referred to in the content.